Macromolecules **2003,** *36,* 6888−6893

Measuring Osmotic Pressure of Poly(ethylene glycol) Solutions by Sedimentation Equilibrium Ultracentrifugation

Christopher B. Stanley and Helmut H. Strey*

Department of Polymer Science and Engineering, University of Massachusetts, Amherst, Massachusetts 01003

Received January 22, 2003; Revised Manuscript Received July 14, 2003

ABSTRACT: The osmotic pressure of aqueous poly(ethylene glycol) (PEG) solutions (400 and 8000 g/mol) was measured by sedimentation equilibrium (SE) ultracentrifugation over a concentration range of 0−50 wt % and over a temperature range of 10−40 °C. We have developed a procedure to cover a large polymer concentration range by performing a series of ultracentrifugation experiments at different loading concentrations. The SE data agreed well with previous measurements made using a vapor pressure osmometer. To facilitate conversion from concentration to osmotic pressure, the data were fitted to multivariable polynomial expressions as a function of the PEG-to-water ratio G and temperature T. The osmotic pressure of PEG solutions decreases with increasing temperature. We attribute this behavior to the release of structured water associated with the PEG chains which compared to bulk water has a lower entropy.

Introduction

The osmotic stress method has been successfully employed to measure intermolecular forces in arrays of biomacromolecules, such as DNA,[1−8] collagen,[9] and polysaccharides,[10] as well as to measure the thermodynamics of conformational changes in enzymes and membrane channels,[11] hydration changes accompanying the binding of oxygen to hemoglobin,[12,13] and thermodynamics of polyelectrolyte−surfactant complex interactions.[14] In this technique, osmotic stress is applied to the system of interest through a neutral osmolyte, such as poly(ethylene glycol). In most cases, the osmolyte size is chosen such that it is prohibited from intercalating with the system of interest, eliminating the need for a dialysis membrane.

To study thermal effects upon forces by the osmotic stress method, the temperature dependence of the osmotic pressure needs to be known. So far, only temperature-dependent osmotic pressure values for PEG 8000[1,15] (formerly known as PEG 6000[16]) have been available. Forces that lead to temperature favored assembly between DNA helices in the presence of $MnCl_2$,[4] collagen triple helices,[9] and hydroxypropylcellulose chains[10] are examples of when such data would be beneficial. In these cases, control over both osmotic pressure and temperature allows for measurement of the entropy and enthalpy of hydration.

The traditional method of measuring osmotic pressure in our concentration range is by vapor pressure osmometry (VPO);[1,15−17] however, temperature control is difficult to achieve using commercial instruments. Also, the typical range of VPO is from 0 to 75 atm in osmotic pressure, and practical sample issues, such as bubbles and high solution viscosity, can adversely affect readings. Other techniques, such as static light scattering and membrane osmometry, require dilute solutions and therefore can only be used at lower osmotic pressures (typically less than 1 atm). In addition, membrane osmometry requires that the osmolyte be large enough to be impermeable to the membrane. We chose analytical ultracentrifugation (AUC) because it allows for osmotic pressure determination with straightforward control of temperature. Others have used this technique for similar measurements involving the osmotic pressure of DNA[18] and the swelling pressure equilibria of gels.[19−21] It also allows us to measure osmotic pressures well above the capabilities of VPO without any complications. The osmolyte concentration gradient created within the AUC cell is typically smaller than the overall concentration range of interest. Therefore, a series of experiments at different starting concentrations had to be performed, covering osmotic pressure differences between 0.2 and 12 atm. The total osmotic pressure as a function of concentration was obtained by merging data sets using a fitting procedure that is described below. Our method is generally applicable to many osmolytes and should be useful in creating a broader, more accurate database for osmotic pressure experiments.[22]

In a sedimentation equilibrium (SE) experiment using the AUC, a radially oriented concentration gradient is established as the sample is centrifuged at a constant angular velocity. There are well-established methods for analyzing this concentration gradient for dilute solutions to determine molecular weight[23] while also accounting for solution nonideality.[24−26] The molecular weight of the solute M_2 can be determined from SE experiments using the following expression

$$\frac{\mathrm{d}\ln c_2}{\mathrm{d}r^2} = \frac{\omega^2}{2}\left(\frac{\partial\rho}{\partial c_2}\right)_\mu \left(\frac{\mathrm{d}\Pi}{\mathrm{d}c_2}\right)^{-1} \quad (1)$$

where c_2 is the concentration of solute, r is the radial distance outward from the center of the centrifuge, ω is the angular velocity, $(\partial\rho/\partial c_2)_\mu$ is the density increment at constant chemical potential of low molecular weight species (i.e., water, c_1, and salt, c_3), and $\mathrm{d}\Pi/\mathrm{d}c_2$ is the derivative of osmotic pressure with respect to c_2. For

---

* To whom correspondence should be addressed: Tel 413-577-1317; Fax 413-545-0082; e-mail strey@mail.pse.umass.edu.

10.1021/ma034079e CCC: $25.00

concentrations approaching zero

$$\frac{\mathrm{d}\Pi}{\mathrm{d}c_2} = \frac{RT}{M_2} \tag{2}$$

giving

$$\frac{\mathrm{d}\ln c_2}{\mathrm{d}r^2} = \frac{M_2\omega^2}{2RT}\left(\frac{\partial\rho}{\partial c_2}\right)_\mu \tag{3}$$

and thus, a plot of ln c_2 vs r^2 will have a slope proportional to M_2.[27] By rewriting eq 1 as

$$\frac{\mathrm{d}c_2}{\mathrm{d}r} = \omega^2\left(\frac{\partial\rho}{\partial c_2}\right)_\mu\left(\frac{\mathrm{d}\Pi}{\mathrm{d}c_2}\right)^{-1}c_2(r)r \tag{4}$$

then multiplying both sides by dΠ/dc_2 and dr, and integrating from the meniscus position r_m to some outward radial position r_i, the difference in osmotic pressure can be found:

$$\Delta\Pi = \omega^2\left(\frac{\partial\rho}{\partial c_2}\right)_\mu\int_{r_\mathrm{m}}^{r_\mathrm{i}}c_2(r)r\,\mathrm{d}r \tag{5}$$

This expression is the same as that obtained by Brian et al.[18] and is the equation necessary to calculate osmotic pressure from SE experiments.

Calculations

Obtaining Concentration from Fringe Displacement. Since PEG does not have a significant absorbance in the UV-to-visible range, we used the Rayleigh interference optical system of the AUC to determine PEG concentrations. With this technique we can determine the difference in solute concentration Δc_2 relative to the concentration at the meniscus $c_2(r_\mathrm{m})$. At low initial concentration the sample can be rapidly centrifuged to obtain meniscus depletion, and then $c_2(r_\mathrm{m}) = 0$ and $c_2(r) = \Delta c_2(r)$. If $c_2(r_\mathrm{m})$ is nonzero, then data fitting is usually necessary. However, because of the relatively high concentrations we are exploring, we have chosen to use a mass balance to calculate $c_2(r_\mathrm{m})$. In general, conservation of mass is not a good assumption in analytical ultracentrifugation experiments because it requires that the entire polymer mass loaded into the ultracentrifuge cell can be detected. Complications arise when the signal at the cell bottom gets noisy due to a steep concentration gradient. This problem was not encountered, most likely because the relatively high loading concentrations used resulted in small concentration gradients. Other methods for calculating meniscus concentration, such as conservation of signal[28] and an extrapolation procedure developed by Creeth and Harding,[29] are usually preferable to a mass balance in conventional analytical ultracentrifugation experiments. As discussed later, the good agreement found between our osmotic pressure data and those made with a vapor pressure osmometer, as well as the independence of our results on the angular velocity, support a mass balance to calculate $c_2(r_\mathrm{m})$ for these experiments.

The raw data, fringe displacement $\Delta m(r)$ vs r, can be converted to the change in concentration $\Delta c_2(r)$ by first converting to the change in refractive index

$$\Delta n(r) = \frac{\Delta m(r)\lambda}{L} \tag{6}$$

where λ is the wavelength of the laser and L is the cell path length, and then dividing by the refractive index increment

$$\Delta c_2(r) = \Delta n(r)\left(\frac{\partial n}{\partial c_2}\right)^{-1} \tag{7}$$

Since $\Delta c_2(r)$ is relative to the concentration at the meniscus, the meniscus concentration must be calculated. This can be done with a mass balance starting with

$$c_2(r) = c_2(r_\mathrm{m}) + \Delta c_2(r) \tag{8}$$

where $c_2(r)$ is the absolute concentration at r, and multiplying both sides by the volume V to get the solute mass

$$x_2(r) = c_2(r_\mathrm{m})V + \Delta c_2(r)V \tag{9}$$

The total (or loading) mass $x_{2,\mathrm{total}}$ can be computed by taking the following integral

$$x_{2,\mathrm{total}} = \int_{r_\mathrm{m}}^{r_\mathrm{b}}x_2(r)\,\mathrm{d}r \tag{10}$$

where r_m and r_b are the meniscus and cell bottom positions, respectively, and the volume can be expressed as

$$V = L({r_\mathrm{b}}^2 - {r_\mathrm{m}}^2)\frac{\pi\alpha}{360} \tag{11}$$

where α is the sector angle of the cell in degrees. This angle was calculated to be 2.42°. Now eq 10 can be used to solve for concentration at the meniscus

$$c_2(r_\mathrm{m}) = \frac{x_{2,\mathrm{total}}}{L({r_\mathrm{b}}^2 - {r_\mathrm{m}}^2)\frac{\pi\alpha}{360}} - \int_{r_\mathrm{m}}^{r_\mathrm{b}}\Delta c_2(r)\,\mathrm{d}r \tag{12}$$

The integral in eq 12 is found by fitting $\Delta c_2(r)$ vs r to a third-order polynomial expression, or a fifth-order polynomial expression if the data have more curvature, and then integrating. It should be noted that this is a nonphysical fit and that sedimentation equilibrium theory yields an exponential expression for the radial dependence of concentration (see eq 3). However, because of the high concentrations being run, there is not much curvature in the concentration gradients established, and so an exponential expression is unsatisfactory. To convert c_2 to wt %, the density data were used to construct plots of wt % vs c_2, where

$$c_2 = \left(\frac{\mathrm{wt}\ \%}{100}\right)\rho(\mathrm{wt}\ \%) \tag{13}$$

and ρ(wt %) is the density at a given wt % for each temperature, and then each curve was fitted to a second-order polynomial expression.

Obtaining Osmotic Pressure. Osmotic pressure is calculated from eq 5 where the integral can be solved by fitting $c_2(r)r$ vs r to either a third- or fifth-order polynomial expression and integrating. Since $\Delta\Pi$ is measured experimentally (Figure 1a), a boundary condition (Π_0) is needed to calculate Π. If meniscus depletion is achieved, the meniscus serves as the boundary condition where $\Pi = 0$ atm at 0 wt %. Alternatively, the curve for the lowest concentration run can be

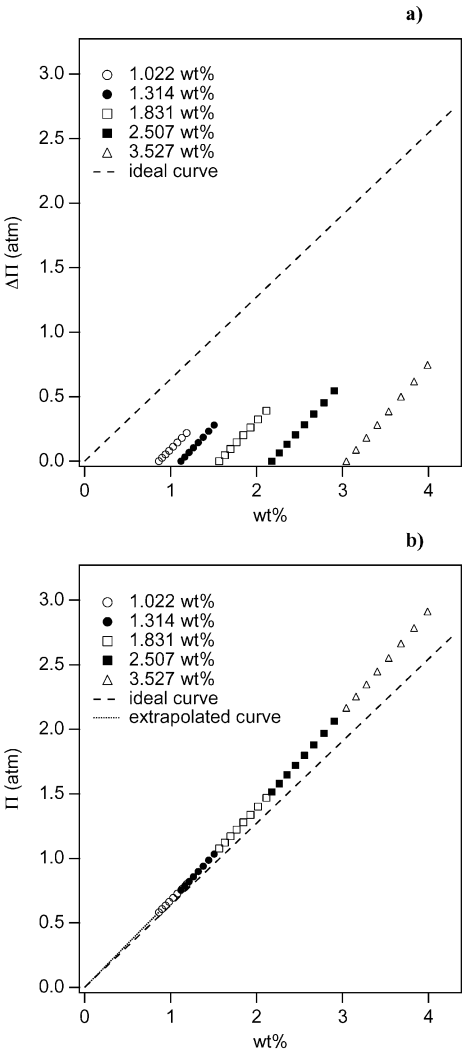

Figure 1. Plot of (a) $\Delta\Pi$ vs wt % for PEG 400 at 20 °C with the corresponding (b) Π vs wt % curve also given to show how the data are shifted. The loading concentration (in wt %) for each sample is listed. Since there are approximately 1500 data points collected for each sample run, only every 200th data point has been plotted for clarity. The ideal curve, using M_n = 407 g/mol, and linear extrapolation from the lowest concentration run to $\Pi = 0$ atm at 0 wt % are also shown.

linearly extrapolated to $\Pi = 0$ atm at 0 wt %, taking error into account. Then all subsequent curves can be shifted to generate a master curve (Figure 1b). When there is a concentration gap between two data sets, we have linearly extrapolated to the midpoint of the gap to determine the osmotic pressure shift of the higher concentration data set.

Experimental Section

Materials. Poly(ethylene glycol) (PEG) of MW 400 (Fluka, Ph Eur grade) and 8000 (Fluka, MicroSelect for Molecular Biology) were used as received. Solutions were prepared by mixing PEG with deionized water (mass/mass). All concentrations are reported as wt % PEG.

Sedimentation Equilibrium. Sedimentation equilibrium measurements were performed using a Beckman Optima XL-I analytical ultracentrifuge, equipped with a Rayleigh interference optical system (λ = 675 nm) and temperature control from 0 to 40 °C. A four-hole Beckman An-Ti 60 rotor with 12 mm Epon charcoal-filled standard double-sector centerpieces and sapphire windows was used. A 3 mm Epon charcoal-filled standard double-sector centerpiece was used in a few runs for comparison.

Table 1. PEG 400 Parameters

T (°C)	$\partial n/\partial c_2$ (mL/g)	$\partial\rho/\partial c_2$	T (°C)	$\partial n/\partial c_2$ (mL/g)	$\partial\rho/\partial c_2$
10	0.137	0.167	35	0.131	0.152
20	0.134	0.162	40	0.129	0.152
30	0.132	0.152			

Table 2. PEG 8000 Parameters

T (°C)	$\partial n/\partial c_2$ (mL/g)	$\partial\rho/\partial c_2$	T (°C)	$\partial n/\partial c_2$ (mL/g)	$\partial\rho/\partial c_2$
10	0.142	0.172	35	0.137	0.157
20	0.140	0.160	40	0.136	0.157
30	0.138	0.158			

The mass of PEG solution loaded into the sample compartment of each cell was used to calculate the meniscus concentration with eq 12. A typical loading mass was approximately 0.4 g (~400 μL), whereas approximately 425 μL of deionized water was loaded into the reference compartment, ensuring that the optical path difference is always taken between the sample and water. Four cells were run simultaneously at 42 000 rpm for both PEG 400 and PEG 8000. Some experiments were performed at lower speeds to determine the effect of hydrostatic pressure on the osmotic pressure. Data were collected at five different temperatures (10, 20, 30, 35, 40 °C) with radial scans taken at constant time intervals. Sedimentation equilibrium was confirmed using a program called MATCH.[30] Typical equilibration time at 42 000 rpm was approximately 72 h for PEG 400 at 20 °C and an additional 24−48 h after each temperature change. At this speed, 144 h was needed for full equilibration of PEG 8000 at 20 °C, and an additional 48−84 h was necessary for equilibration after each temperature change. Some runs were concluded by reequilibrating at the starting temperature (20 °C) to confirm that neither the duration of the run nor the temperature history had an effect on the measured osmotic pressure. The radial scans for each sample run contained about 1500 data points. For clarity, some figures show data sets with only every 200th point plotted, and this has been stated in the corresponding figure caption.

Density and Refractometry Measurements. The density and refractive index of PEG 400 and PEG 8000 solutions were measured as functions of c_2 and temperature T to obtain $\partial\rho(T)/\partial c_2$and $\partial n(T)/\partial c_2$, respectively (see Tables 1 and 2), which are used to calculate $\Delta\Pi(T)$ and $\Delta c_2(T)$ by eq 5 and eq 7, respectively. Density was measured using a series of PEG 400 and PEG 8000 solutions (prepared in 10 wt % increments from 0 to 50 wt %) along with a 2 mL round-bottom flask and a water bath. On the basis of reference values for the density of water as a function of temperature,[31] a correction factor was applied to the solution densities at each measured temperature to correct for any changes in the containing volume of the volumetric flask with temperature. This method is not as accurate as a U-tube densitometer, but we are able to calculate $\partial\rho(T)/\partial c_2$ to ±0.005, resulting in about 3% relative error in $\Delta\Pi$. Refractive index measurements were made using an Abbe refractometer containing a prism assembly connected to a water bath. The refractometer measures the refractive index at 589 nm while the ultracentrifuge interference optics has a wavelength of 675 nm. We assume the wavelength dependence to be negligible and estimate an error in $\partial n(T)/\partial c_2$ of ±0.001 mL/g. This results in a relative error in Δc_2 of less than 1%.

Results and Discussion

Osmotic Pressure of PEG. When shifting the data in osmotic pressure to obtain the master curve, the lowest concentration data set is used to linearly extrapolate to 0 wt % at $\Pi = 0$ atm (Figure 1b). The slope of this extrapolation for PEG 400 at 20 °C gives $\partial\Pi/\partial c_2$ = 6.8 J/g, and this corresponds to an apparent molecular weight M_{app} = 360 g/mol using eq 2. By fast atom bombardment (FAB) mass spectrometry (JMS700 MStation, JEOL) the number-average molecular weight M_n = 407 g/mol (PDI = 1.07), which was used to draw the

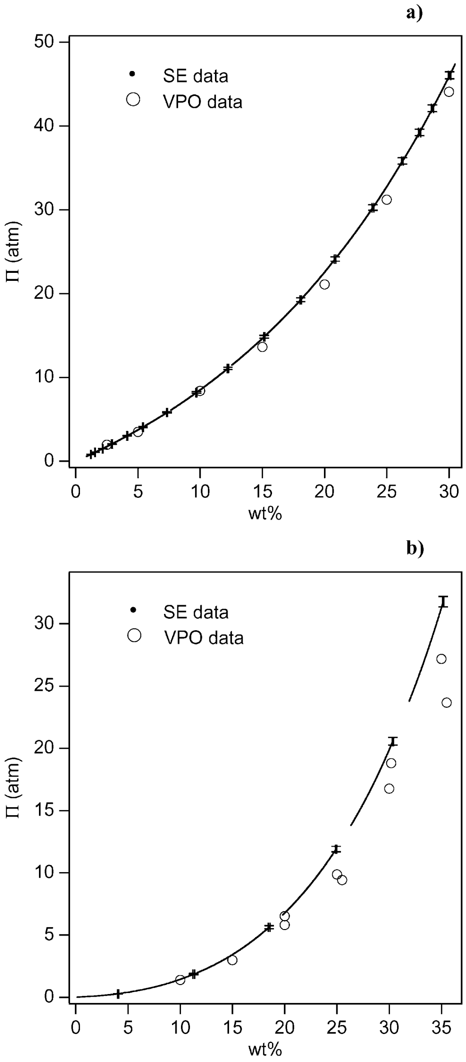

Figure 2. Plots of Π vs wt % for (a) PEG 400 and (b) PEG 8000 at 20 °C as determined by SE compared to the VPO data for PEG 400 and 8000, respectively, at 20 °C. Good agreement is found between the two methods for PEG 400 while there is some deviation between the two methods for PEG 8000. This is attributed to a different supplier and grade of PEG 8000 used in the VPO experiments.

ideal solution curve in Figure 1a,b for comparison. The osmotic pressure for PEG 400 is observed to quickly diverge from ideality as concentration increases.

Comparing the osmotic pressure data obtained by SE for PEG 400 at 20 °C to that obtained previously by Parsegian et al. using vapor pressure osmometry (VPO) at the same temperature[1,22] (Figure 2a), it can be seen that there is good agreement between the two techniques. At higher wt % PEG, the VPO data are slightly lower in osmotic pressure than the SE data, but the difference does not exceed 7% relative to the SE data. The osmotic pressure of PEG 8000 obtained by SE and that previously obtained by VPO[22] (Figure 2b) do not agree as well as the data for PEG 400. However, it should be noted that the PEG 8000 used in the VPO measurements is from a different supplier and of a different grade. Therefore, polydispersity and impurities may contribute to the observed differences.

The temperature dependence of Π for PEG 400 and 8000 is shown in Figure 3. Error bars have been omitted from these figures for clarity. After accounting for the error by using a mass balance to determine concentration, as well as the error in $\partial n/\partial c_2$ and $\partial \rho/\partial c_2$, the relative error in wt % PEG is no more than 0.1% and does not exceed 1% in Π. These errors are less than those in the corresponding relative variables (Δc_2 and $\Delta\Pi$, respectively) because the data are shifted to an absolute scale. The tabulated form of the Π data for PEG 400 and PEG 8000 is given in Tables 3 and 4, respectively. The osmotic pressure is found to be relatively independent of temperature up to about 15 wt % for PEG 400 and up to about 10 wt % for PEG 8000. The difference in values found for PEG 400 (up to 15 wt %) with changing

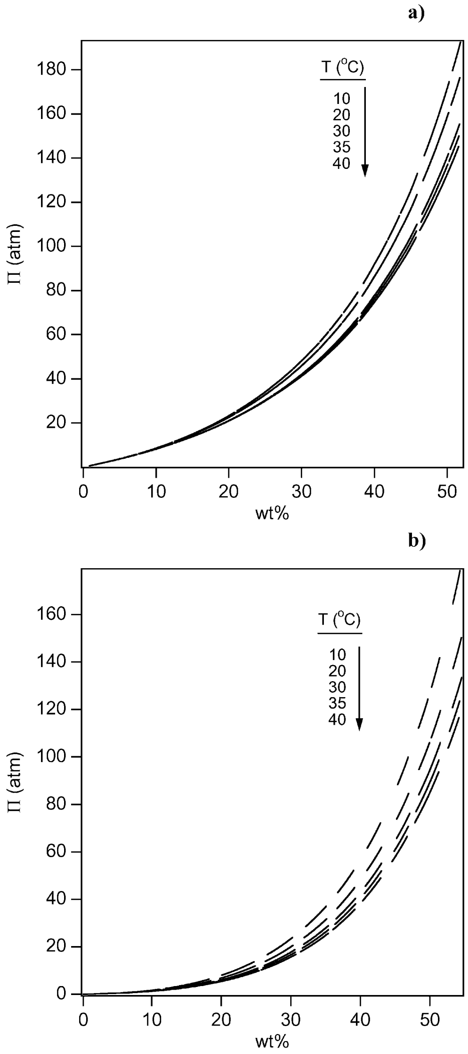

Figure 3. Temperature dependence of Π for (a) PEG 400 and (b) PEG 8000. Error bars have been omitted for clarity. Osmotic pressure is observed to decrease with increasing temperature. This effect becomes more pronounced at higher concentrations.

Table 3. PEG 400 Osmotic Pressure Data

	Π (atm)				
wt %	10 °C	20 °C	30 °C	35 °C	40 °C
5	3.69	3.74	3.65	3.70	3.71
10	8.55	8.52	8.17	8.24	8.23
15	14.9	14.7	13.8	13.9	13.8
20	23.2	22.6	21.0	21.0	21.0
25	34.0	32.8	30.2	30.0	30.0
30	48.1	45.9	42.0	41.5	41.2
35	66.7	63.1	57.3	56.4	55.6
40	91.9	86.3	77.7	76.2	74.8
45	125	117	104	102	99.6
50	172	159	141	137	133

Table 4. PEG 8000 Osmotic Pressure Data

	Π (atm)				
wt %	10 °C	20 °C	30 °C	35 °C	40 °C
5	0.445	0.407	0.385	0.373	0.367
10	1.63	1.44	1.31	1.25	1.19
15	3.95	3.43	3.08	2.89	2.74
20	7.91	6.78	6.04	5.66	5.33
25	14.1	12.0	10.7	10.0	9.43
30	23.3	19.9	17.6	16.6	15.6
35	36.7	31.3	27.8	26.1	24.7
40	56.7	48.2	42.9	40.4	38.3
45	85.8	72.5	64.5	60.8	57.8
50	126	106	94.3	89.2	84.8
54	173	144	127	121	115

temperature (see Table 3) is within the error in Π. Above these concentrations, the observed decrease in osmotic pressure with increasing temperature is attributed to the release of structured water molecules from the PEG. The positive entropy difference between bulk and structured water drives this release.

Similar to Michel and Kaufmann,[15,16] the Π curves for PEG 400 (Figure 3a) can be fitted to a multivariable polynomial expression as a function of the PEG-to-water ratio G, where G = wt %/(100 − wt %), and T to obtain

$$\Pi = -1.36G^2T + 117.2G^2 + 67.8G \qquad (14)$$

which is valid over a range of $0 < G < 1.08$ (0 < wt % < 52) and $10 < T < 40$ °C. This equation simplifies the conversion from wt % to Π at a given temperature and is found to have an average error of 2% compared to the actual data. The maximal error is 6%, which occurs for calculations near 1 wt % at 10 °C, and the error does not exceed 4% above 10 wt % for all temperatures. Likewise, the Π data for PEG 8000 (Figure 3b) can be fitted to the following expression

$$\Pi = -1.38G^2T + 134.3G^2 + 3.0G \qquad (15)$$

which is valid for $0.11 < G < 1.18$ (10 < wt % < 54) and $10 < T < 40$ °C. This equation has an average error of 4% compared to the actual data. The maximal error is 15%, and the error does not exceed 9% above 20 wt % for all temperatures. However, because the above equation is not reliable for concentrations below 10 wt %, another fit was made for $0.03 < G < 0.25$ (3 < wt % < 20) and $10 < T < 40$ °C

$$\Pi = -1.29G^2T + 127.6G^2 + 2.0G \qquad (16)$$

This equation has an average error of 4% and a maximal error of 25%, and the error does not exceed 19% above 4 wt % for all temperatures.

Hydrostatic Pressure. The effect of hydrostatic pressure P on the osmotic pressure is a potential concern in these SE experiments, especially since P is proportional to (rpm)^2. It has even been suggested that P can change the solubility of PEG.[11] At 42 000 rpm a pressure difference $\Delta P \approx 150$ atm exists between the cell bottom and meniscus. To investigate changes in Π with P, several runs with PEG 8000 were performed at slower rotor speeds and at 20 °C to compare to the 42 000 rpm data at this temperature. Runs in the 1−25 wt % range at 20 000 rpm, where $\Delta P \approx 34$ atm, were used to construct a master curve which showed no significant deviation from the original master curve obtained at 42 000 rpm (Figure 4). The independence of Π on speed demonstrates that P does not significantly affect Π, at least for $P < 150$ atm. There are larger gaps between individual data sets collected at lower speeds that require further extrapolation when determining the shift in Π. We expect that the two curves would show even better agreement if more data sets were collected over this concentration range at this speed. Other runs in the 45−50 wt % range were performed at 10 000 and 5000 rpm (not shown). The data obtained at 10 000 rpm seemed to have the same slope as at 42 000 rpm, but it was difficult to compare because the error in wt % was almost as large as the concentration gradient formed within the cell. The 5000 rpm data could not be compared at all because the error in wt % was larger than the concentration gradient formed. Also, several runs with PEG 400 in the 35−45 wt % range were performed at 33 600 rpm and 20 °C (not shown) and were found to agree well with the corresponding data at 42 000 rpm. The comparisons made with VPO data are also a good indication that hydrostatic pressure does not influence osmotic pressure significantly.

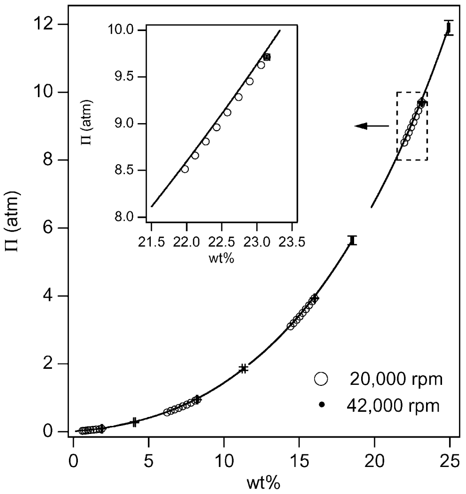

Figure 4. Plots of Π vs wt % for PEG 8000 at 20 °C and speeds of 20 000 and 42 000 rpm. Only every 200th data point, along with the last data point, for each sample run at 20 000 rpm has been plotted for clarity. The data at 20 000 rpm have been used to create a master curve up to 25 wt %. This curve follows the original master curve generated from data collected at 42 000 rpm (see inset for a closer comparison). Since hydrostatic pressure P is proportional to (rpm)^2, the independence of Π on angular velocity shows that P is not significant at least up to $P \approx 150$ atm.

Conclusions

We have used sedimentation equilibrium to measure the effect of temperature on the osmotic pressure of aqueous solutions of PEG 400 and 8000. As temperature increases, the osmotic pressure of PEG decreases due to the release of structured water molecules from the polymer chain. No significant differences in osmotic pressure were observed with changes in hydrostatic pressure up to $P \approx 150$ atm. Using our method, it should be possible to measure the temperature dependence of osmotic pressure for other molecular weights of PEG as well as for other osmolytes. It should also permit direct measurement of the effect of added salts on the osmotic pressure of those osmolytes. Since low molecular weight species, such as salts, do not form a concentration gradient in a centrifugal field, the osmotic pressure of the osmolyte can be measured at constant salt activity. Only interactions between the salt and osmolyte through the change in osmolyte osmotic pressure are observed. This represents a major advantage of sedimentation equilibrium over vapor pressure osmometry for which the salt and osmolyte osmotic pressures are additive. These measurements should prove useful in expanding the versatility of the osmotic stress technique.

Acknowledgment. We thank Michael Leonard for helpful comments on the manuscript and Stephen Eyles for collecting the mass spectrum of PEG 400. This material is based on work supported by the National Science Foundation under Career Award DMR-9984427 and Instrumentation Award DMR-9975762. We also acknowledge support from the Materials Research Science and Engineering Center at the University of Massachusetts (DMR-0213695).

References and Notes

(1) Parsegian, V. A.; Rand, R. P.; Fuller, N. L.; Rau, D. C. *Methods Enzymol.* **1986**, *127*, 400.
(2) Podgornik, R.; Rau, D. C.; Parsegian, V. A. *Macromolecules* **1989**, *22*, 1780.
(3) Podgornik, R.; Parsegian, V. A. *Macromolecules* **1990**, *23*, 2265.
(4) Leikin, S.; Rau, D. C.; Parsegian, V. A. *Phys. Rev. A* **1991**, *44*, 5272.
(5) Podgornik, R.; Strey, H. H.; Gawrisch, K.; Rau, D. C.; Rupprecht, A.; Parsegian, V. A. *Proc. Natl. Acad. Sci. U.S.A.* **1996**, *93*, 4261.
(6) Strey, H. H.; Parsegian, V. A.; Podgornik, R. *Phys. Rev. Lett.* **1997**, *78*, 895.
(7) Strey, H. H.; Parsegian, V. A.; Podgornik, R. *Phys. Rev. E* **1999**, *59*, 999.
(8) Strey, H. H.; Wang, J.; Podgornik, R.; Rupprecht, A.; Yu, L.; Parsegian, V. A.; Sirota, E. B. *Phys. Rev. Lett.* **2000**, *84*, 3105.
(9) Leikin, S. L.; Rau, D. C.; Parsegian, V. A. *Proc. Natl. Acad. Sci. U.S.A.* **1994**, *91*, 276.
(10) Bonnet-Gonnet, C.; Leikin, S.; Chi, S.; Rau, D. C.; Parsegian, V. A. *J. Phys. Chem. B* **2001**, *105*, 1877.
(11) Parsegian, V. A.; Rand, R. P.; Rau, D. C. *Methods Enzymol.* **1995**, *259*, 43.
(12) Colombo, M. F.; Rau, D. C.; Parsegian, V. A. *Science* **1992**, *256*, 655.
(13) Rand, R. P. *Science* **1992**, *256*, 618.
(14) Leonard, M.; Hong, H.; Easwar, N.; Strey, H. H. *Polymer* **2001**, *42*, 5823.
(15) Michel, B. E. *Plant Physiol.* **1983**, *72*, 66.
(16) Michel, B. E.; Kaufmann, M. R. *Plant Physiol.* **1973**, *51*, 914.
(17) Michel, B. E. *Plant Physiol.* **1972**, *50*, 196.
(18) Brian, A. A.; Frisch, H. L.; Lerman, L. S. *Biopolymers* **1981**, *20*, 1305.
(19) Borchard, W.; Cölfen, H. *Makromol. Chem., Macromol. Symp.* **1992**, *61*, 143.
(20) Hinsken, H.; Borchard, W. *Colloid Polym. Sci.* **1995**, *273*, 913.
(21) Cölfen, H.; Borchard, W. *Macromol. Chem. Phys.* **1995**, *196*, 3469.
(22) Updated data can be found on the Internet at: http://aqueous.labs.brocku.ca.
(23) Yphantis, D. A. *Biochemistry* **1964**, *3*, 297.
(24) Roark, D. E.; Yphantis, D. A. *Biochemistry* **1971**, *10*, 3241.
(25) Yphantis, D. A.; Roark, D. E. *Biochemistry* **1972**, *11*, 2925.
(26) Stafford, W. F.; Yphantis, D. A. *Biophys. J.* **1972**, *12*, 1359.
(27) Eisenberg, H. *Biological Macromolecules and Polyelectrolytes in Solutions*; Oxford University Press: New York, 1976.
(28) Minton, A. P. In *Modern Analytical Ultracentrifugation*; Schuster, T. M., Laue, T. M., Eds.; Birkhäuser: Boston, 1994.
(29) Creeth, J. M.; Harding, S. E. *J. Biochem. Biophys. Methods* **1982**, *7*, 25.
(30) Yphantis, D. A.; Lary, J. W. 0.99 ed.; 1999 (available for download at: http://www.ucc.uconn.edu/~wwwbiotc/AUFFT-P.HTML or ftp://spin6.mcb.uconn.edu).
(31) Lide, D. R., Ed. *Handbook of Chemistry and Physics*, 79th ed.; CRC Press: Boston, 1998.

MA034079E